RAI Volume 3, Chapter 2.2.1.2.1, Sixth Set, Number 4:

Describe how uncertainties in the stress-strain relationships for the Topopah Spring lower lithophysal tuff have been characterized and considered in the UDEC-Voronoi model. Clarify how post-peak strains are represented in the UDEC model for each rock-mass category, such that the effects of brittle deformation have not been underestimated.

Basis: Although the single comparison between the lithophysal tuff and UDEC calculation for stress-strain characteristics does show a calculated response that is more brittle than exhibited by the laboratory experiment (DOE, 2009, RAI-3), this information does not address the range of characteristics represented by the five lithophysal rock-mass categories used in the UDEC analyses. Additionally, strength characteristics for only six samples from the Topopah Spring lower lithophysal tuff are reported in BSC (2007, Table 6-69). Staff cannot determine if these six samples are appropriately representative of the range of strength characteristics needed to support the UDEC analyses (cf. BSC, 2004, Figure 7-16).

1. RESPONSE

1.1 INTRODUCTION

In the drift stability analyses, the range in the mechanical behavior of the lithophysal rock mass was represented by five rock mass categories, as shown in SAR Figure 2.3.4-30. By utilizing these five rock mass categories and a bounding approach to modeling the rock mass response, the variability and uncertainties of the laboratory and field data were encompassed in the analyses. The drift stability was analyzed using five different Universal Distinct Element Code (UDEC) Voronoi block models with stress-strain relations calibrated to each lithophysal rock mass category. The laboratory testing data for these rock masses indicate good correlation between the lithophysal porosity and the rock mass quality, so the five rock mass categories represent the range in rock mass quality and lithophysal porosities. Compared to porosity, the other factors (e.g., fracturing or specific unit, such as upper or lower lithophysal) have a second-order effect on strength and stiffness. The six tests on large-diameter lower lithophysal samples were sufficient to demonstrate that mechanical behavior of the lower lithophysal tuff is a function of porosity, similar to the way that porosity affects the behavior of the upper lithophysal tuff. Thus, lower and upper lithophysal tuffs were not considered differently in the analyses. More detailed discussion on the effect of porosity on mechanical behavior of the lithophysal rock mass is provided in Section 1.2.1 of this response.

The variability and the uncertainties in the stiffness and strength of both upper and lower lithophysal rock mass were addressed by: (1) consideration of five rock mass categories in the drift stability analysis, and (2) consideration of the lower bound strength envelope (see BSC 2004, Section 6.4.2.2.3.1, and the response to RAI 3.2.2.1.2.1-6-003). Because the post-peak material response has an important effect on stability of the tunnels in the overstressed rock, the UDEC Voronoi block model used for drift stability analyses was calibrated to bound the brittleness of the lithophysal rock mass observed from the experimental data. The uncertainties in the post-peak response of both upper and lower lithophysal were addressed by ensuring the model response for a given rock mass category is more brittle than any tested rock response that is closely related to that category. Any assumption of perfectly brittle behavior of the rock around the drift is unrealistic. This is borne out by the behavior observed in Yucca Mountain tunnels, natural analogues, and experience with excavation of underground structures (the natural analogues are discussed in detail in BSC 2004, Appendix G). The discussion regarding brittleness (or ductility) of the lithophysal rock is provided in Section 1.2.2. In Section 1.3, the stress-strain curves obtained from tests on large-diameter (10.5- and 11.4-inch) samples of the lithophysal rock mass are compared with stress-strain curves generated during calibration of the UDEC Voronoi block model to five different lithophysal rock mass categories.

1.2 CHARACTERIZATION OF MECHANICAL PROPERTIES OF THE LITHOPHYSAL TUFF

The foundation for understanding the post-peak behavior of the Yucca Mountain tuffs is the database of tuff mechanical properties from laboratory experiments that have been performed.

From the results of many experiments on Yucca Mountain tuff samples in the 1980s and 1990s, relationships were developed between the rock physical properties and the lab-measured mechanical properties. The most distinct and important relationships discovered were the dependence of ultimate intact rock strength and Young's modulus on the total porosity of the rock (Price and Bauer 1985; Price et al. 1994). In addition, empirical equations relating tensile strength and p- and s-wave velocities with porosity were also developed (Price et al. 1996). These initial relationships all came from data gathered during experiments on nonlithophysal tuffs from Yucca Mountain.

1.2.1 Dependence of Mechanical Properties of Lithophysal Tuff on Porosity

Lithophysae are cavities (sometimes also referred to as lithophysal cavities or lithophysal voids) in the welded tuffs that can range in size from a few millimeters up to a meter or more. These features are formed by volatiles trapped in the ash-flow tuff during the cooling phase following emplacement (Ross and Smith 1961).

Within Yucca Mountain, the upper lithophysal zone of the Topopah Spring tuff has smaller lithophysal voids (generally a few millimeters to several centimeters) than the lower lithophysal zone (which can range in size up to almost a meter). As a result, with the sample size limitations, it has been easier to characterize the mechanical properties of the upper lithophysal zone in the laboratory.

In order to confirm that the larger pores in the lithophysal samples caused the same reduction of strength and Young's modulus observed in the nonlithophysal samples, the lab mechanical property results from an early study on large samples of lithophysal tuff were compared with the results from the nonlithophysal tuffs (Price and Bauer 1985). In order to do this, scale had to be considered because the earlier experiments on nonlithophysal tuffs were conducted on much smaller (1- to 2-inch diameter) samples than the experiments on lithophysal tuffs. Considering the scale dependence on strength (Price 1986), the comparison was made between the ultimate strengths from 10 experiments on large (10.5-inch diameter) lithophysal samples, from the upper lithophysal zone, and the existing strength-porosity relationship. It was found that the ultimate strength versus porosity results from the lithophysal samples were within the inherent scatter of the nonlithophysal tuffs (Price 1993), confirming that as long as scale is taken into consideration, the larger porosity from lithophysae could be considered to affect mechanical properties with the same relationships developed from samples with smaller-sized porosity. Also, the test data on the upper and lower lithophysal follow the same trend. Thus, the upper and lower lithophysal tuffs have not been differentiated in the drift stability analyses, and the five categories used in the analyses represent the lithophysal rock mass with different porosities and different mechanical properties.

The variability and uncertainty in the loading part of the stress-strain curves (i.e., stiffness and strength) are subject of extensive investigation as documented in *Drift Degradation Analysis* (BSC 2004, Section E4.1.4.1). The range in variability in stiffness and strength (BSC 2004, Figure E-13) is completely covered by five rock mass categories for the mean and lower bound strength envelopes. The sensitivity of the drift stability predictions to five rock mass categories is discussed in Section 6.4.2 of *Drift Degradation Analysis* (BSC 2004). The sensitivity of the drift stability predictions to uncertainty in the strength for a given stiffness is discussed in Section 6.4.2.2.3.1 of *Drift Degradation Analysis* (BSC 2004) and in the response to RAI 3.2.2.1.2.1-6-003. Sensitivity of the model predictions to the variability and uncertainty in the strength and stiffness is not discussed any further in this response. The variability and the uncertainty in the post-peak part of the stress-strain curve for the lower and upper lithophysal rock and its representation in the UDEC Voronoi block model is discussed in the following sections.

1.2.2 Post-Peak Response and Brittleness of Lithophysal Tuff

In general, as mechanical load is applied to a sample, the stress-strain curves for the lithophysal tuffs are initially linear, then the stress-strain behavior becomes nonlinear (concave-downward) somewhere between 80% and 100% of peak stress. The samples do not lose their strength immediately, but continue to strain-soften (reflected in decreasing strength, concave-downward curves), then eventually lose complete strength at some strain level significantly larger than the strain at peak stress (ultimate strength).

The high-porosity, lithophysal tuff samples deform by fracturing. In these tuffs, cracks propagate from one lithophysal cavity to another within the low-porosity, very strong, highly welded tuff between the lithophysae. These discontinuous fractures begin forming at a stress level above 80% of peak stress. In fact, the acoustic emissions from the fracturing process are audible without amplification during the experiment. Each fracture creates a local failure of material; however, the strength of the macroscopic sample continues to increase until there are enough fractures that the sample begins to lose load-bearing capability (i.e., at the peak stress). Following the peak stress, these samples do not completely lose strength, however, but the process of localized (lithophysae-to-lithophysae) fracturing continues to accumulate damage. As a result, the sample loses strength in a gradual manner, because the increasing numbers of fractures do not immediately form a continuous fracture, causing macroscopic failure of the sample (i.e., a complete loss of strength), until a larger total strain accumulation is reached.

As discussed, the predominant deformation mechanism in the lithophysal tuffs (under repository-type pressure and temperature conditions) is brittle fracturing. However, these tuffs exhibit some ductility (defined as the material property of being able to "sustain permanent deformation without losing its ability to resist load" (Jaeger and Cook 1976, p.80)) in part of the pre-peak and the post-peak stress-strain curves.

In summary, modeling the stress-strain behavior of the lithophysal tuffs with a more brittle post-peak behavior than that observed in the laboratory will tend to overestimate rockfall. This is because the lithophysal tuffs exhibit strain-softening as shown in figures in the following section, and maintain some ability to resist load after the peak stress is reached.

1.3 APPROXIMATION OF LITHOPHYSAL POST-PEAK RESPONSE IN UDEC VORONOI BLOCK MODEL

Because post-peak response of the brittle rocks is typically much more random than the elastic (pre-peak) portion of the stress-strain curve, the UDEC Voronoi block model was not calibrated to post-peak test data. The UDEC Voronoi block model matches the stiffness and strength of the five lithophysal rock mass categories. However, as shown below in comparisons between lab data and model representations, the model for all five categories is calibrated in such a way that it bounds brittleness observed from all test data (i.e., the model exhibits more brittle response than indicated by any data). In this manner, the range in mechanical data is accounted for and bounded in the drift stability analyses.

Comparisons of unconfined compression data obtained from different tests on large-diameter lithophysal samples with UDEC Voronoi block stress-strain curves for the five lithophysal rock mass categories are shown in Figures 1 through 10. As discussed in Section 1.1, the same model is used for both upper and lower lithophysal rock masses.

A comparison of the experimental stress-strain curves for all of the saturated 10.5-inch-diamater samples of the upper lithophysal tuff with numerical curves is shown in Figure 1. Note that test data on saturated samples typically had lower strengths than comparable unsaturated samples and the model curves. The saturated samples fell near the lower bound of the strength envelope defining the mechanical property ranges for the five rock mass categories (as shown in SAR Figure 2.3.4-30). Because the UDEC Voronoi data in these plots are for the mean relation between strength and stiffness, the model curves typically show higher strength for the same stiffness. (Development of the relation between strength and stiffness, shown, for example, in Figure E-13, is discussed in BSC 2004, Section E4.1.4.1.) However, comparison of the post-peak softening parts of the stress-strain curves clearly indicates a more brittle model response. That conclusion is more obvious in Figures 2 through 4, in which the curves are roughly divided into ranges of categories and compared with corresponding numerical curves. Brittleness of the UDEC Voronoi block model changes between different categories. As typically observed in rocks, the weaker, less-stiff rocks are more ductile (e.g., Category 1).

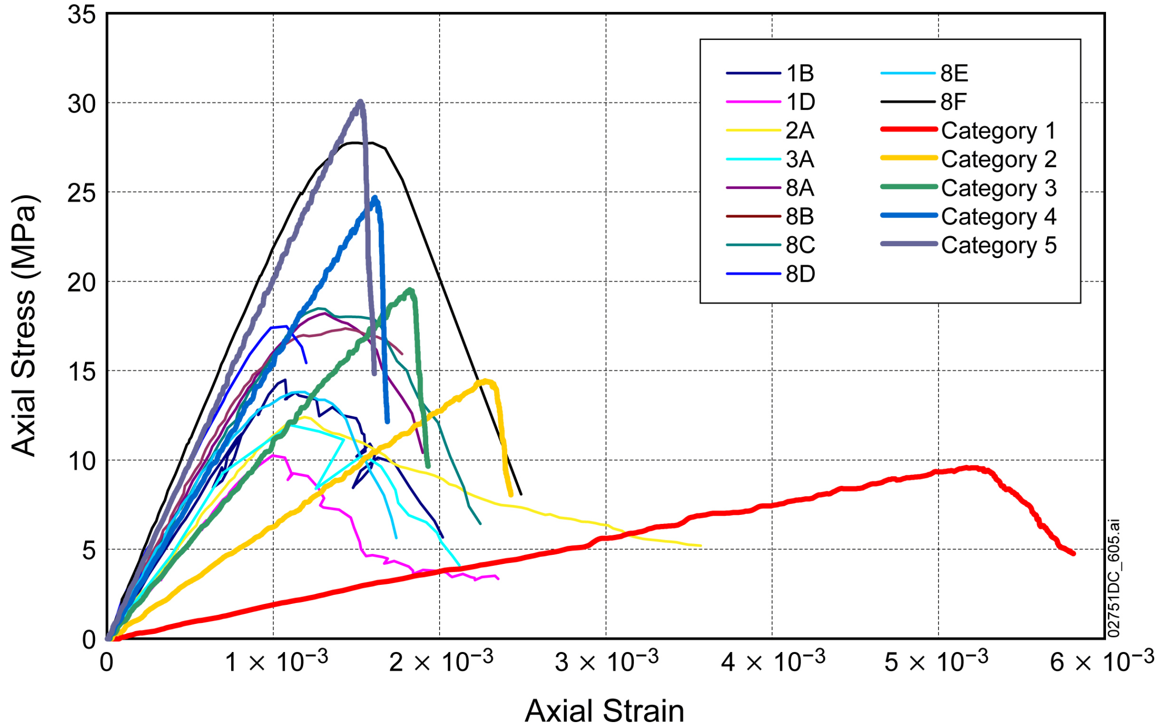

NOTE: Thick lines represent UDEC Voronoi block model data; thin lines represent the experimental data.

Figure 1. Comparison of Stress-Strain Curves Obtained from Tests on 10.5-Inch-Diameter Upper Lithophysal, Saturated Samples with Responses of the Calibrated UDEC Voronoi Block Model

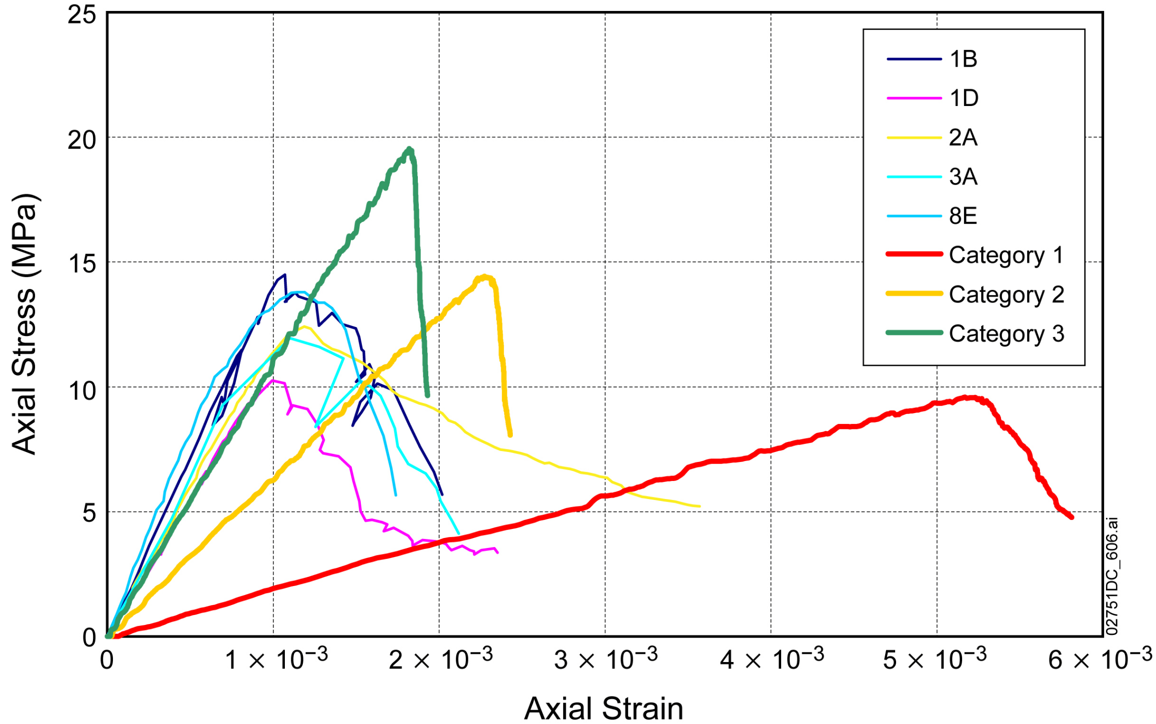

NOTE: Thick lines represent UDEC Voronoi block model data; thin lines represent the experimental data.

Figure 2. Comparison of Stress-Strain Curves Obtained from Tests on 10.5-Inch-Diameter Upper Lithophysal, Saturated Samples with Responses of the Calibrated UDEC Voronoi Block Model for the Range of Rock Mass Qualities Corresponding to Categories 1, 2, and 3

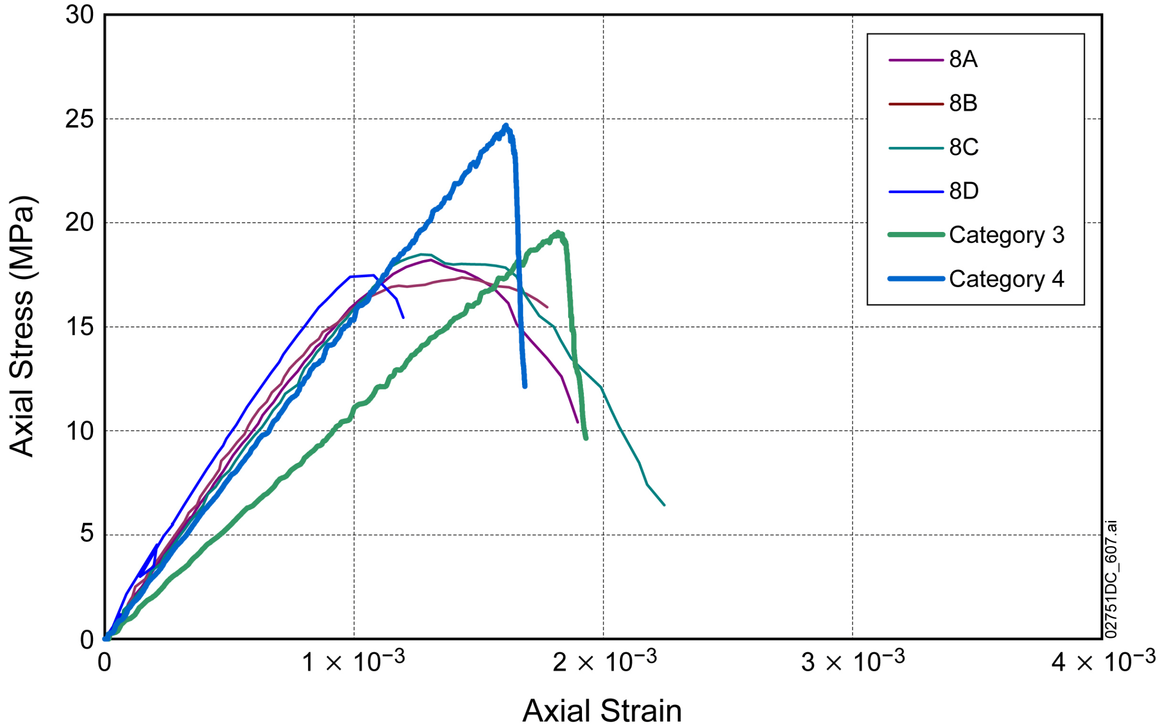

NOTE: Thick lines represent UDEC Voronoi block model data; thin lines represent the experimental data.

Figure 3. Comparison of Stress-Strain Curves Obtained from Tests on 10.5-Inch-Diameter Upper Lithophysal, Saturated Samples with Responses of the Calibrated UDEC Voronoi Block Model for the Range of Rock Mass Qualities Corresponding to Categories 3 and 4

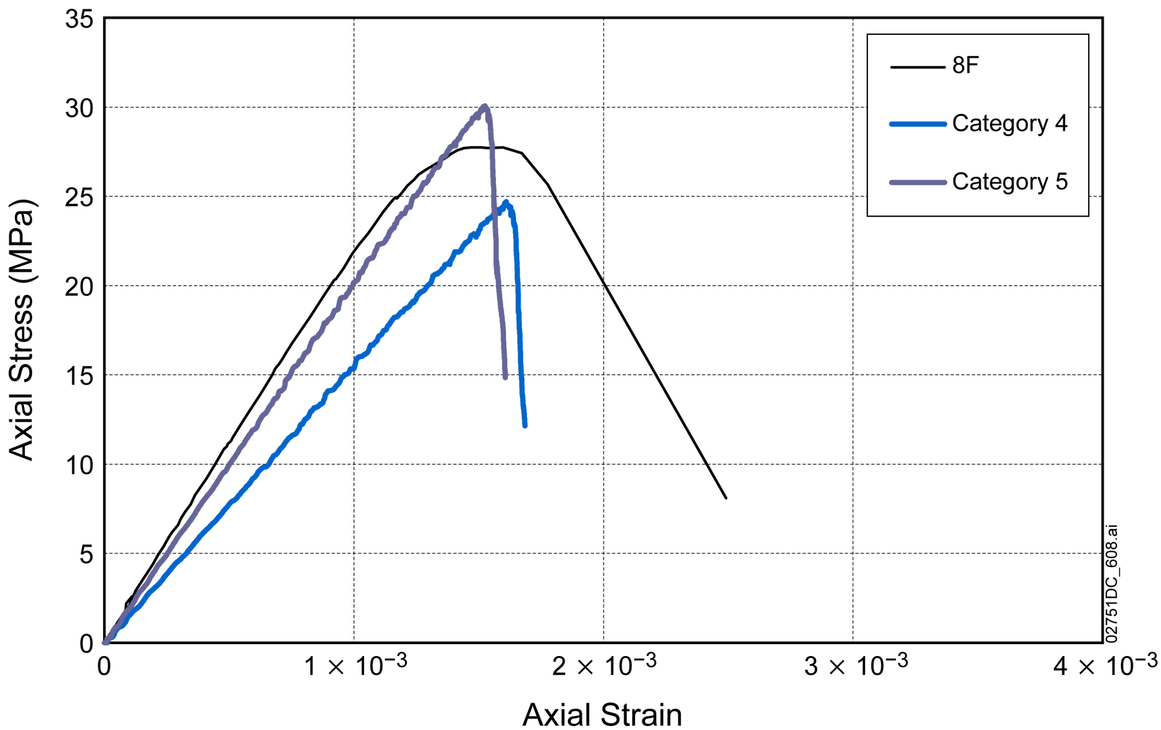

NOTE: Thick lines represent UDEC Voronoi block model data; thin lines represent the experimental data.

Figure 4. Comparison of Stress-Strain Curves Obtained from Tests on 10.5-Inch-Diameter Upper Lithophysal, Saturated Samples with Responses of the Calibrated UDEC Voronoi Block Model for the Range of Rock Mass Qualities Corresponding to Categories 4 and 5

The comparison between six lower lithophysal experimental curves and the numerical curves is shown in Figure 5. Again, the test and numerical curves do not generally coincide because the numerical curves are for the mean relation between the strength and stiffness (BSC 2004, Figure E-18), while particular data (curves) show some scatter around the mean relation. However, although the test data exist for relatively small strains beyond the strain that corresponds to the peak strength, it is clear from the comparisons, based on the shapes of the curves and recorded post-peak response, that the UDEC Voronoi block model bounds (overestimates) brittleness of the all test data. Furthermore, the numerical model exhibits stiffer and weaker material response than corresponding lower lithophysal curves, indicating that five lithophysal rock mass categories, as represented in the UDEC Voronoi block model, conservatively bound the stresses and damage that would occur around the emplacement drift in the lower lithophysal units during the thermal cycle.

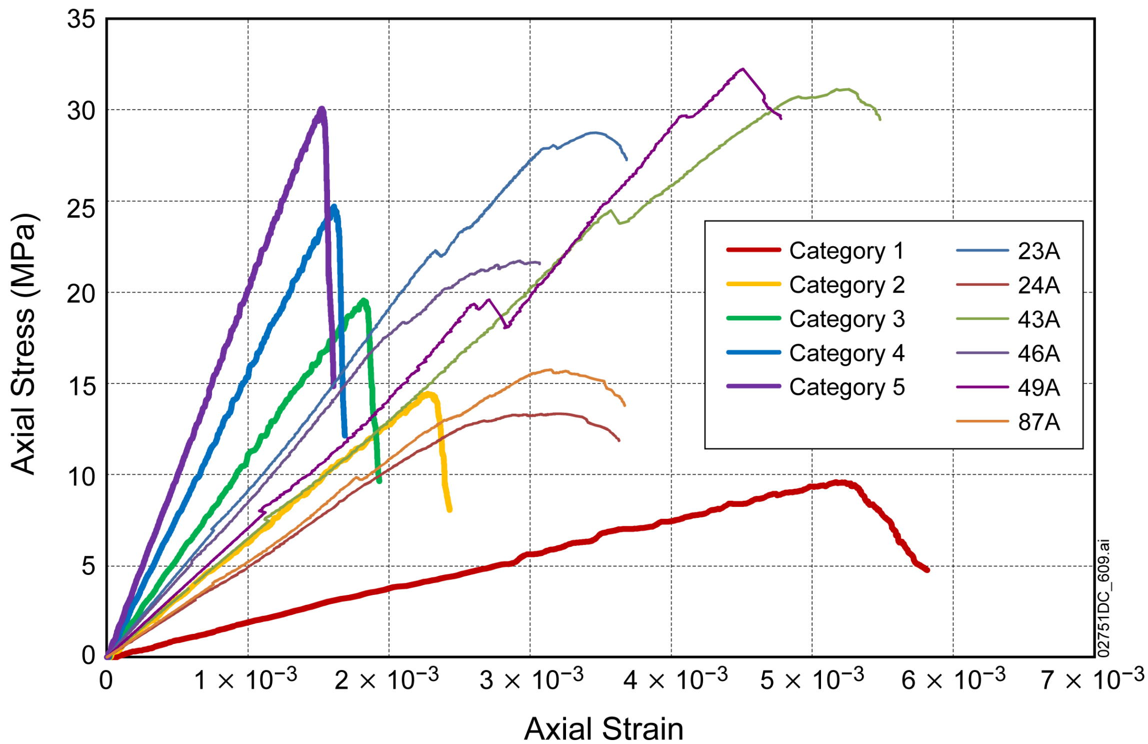

NOTE: Thick lines represent UDEC Voronoi block model data; thin lines represent the experimental data.

Figure 5. Comparison of Stress-Strain Curves Obtained from Tests on 11.4-Inch-Diameter Lower Lithophysal Samples with Responses of the Calibrated UDEC Voronoi Block Model (87A – 24°C saturated; 23A, 24A, 46A – 24°C room dry; 43A – 200°C dry; 49A – 195°C dry)

Finally, the test data on 11.4-inch-diameter samples from the upper lithophysal tuff are compared with numerical stress strain curves. All curves are presented in Figure 6. Figures 7 through 10 show comparison of numerical and test data divided in smaller rock mass quality ranges. With the exception of the Category 1, which represents small volumes of high-porosity lithophysal rock mass (less than 5% according to BSC 2004, Table 6-41 and Figure 6-115), the UDEC Voronoi block model accurately represents the test data. Although a significant portion of the softening curve is not included in all of the experimental data, it is clear that the numerical curves bound brittleness of the tested samples.

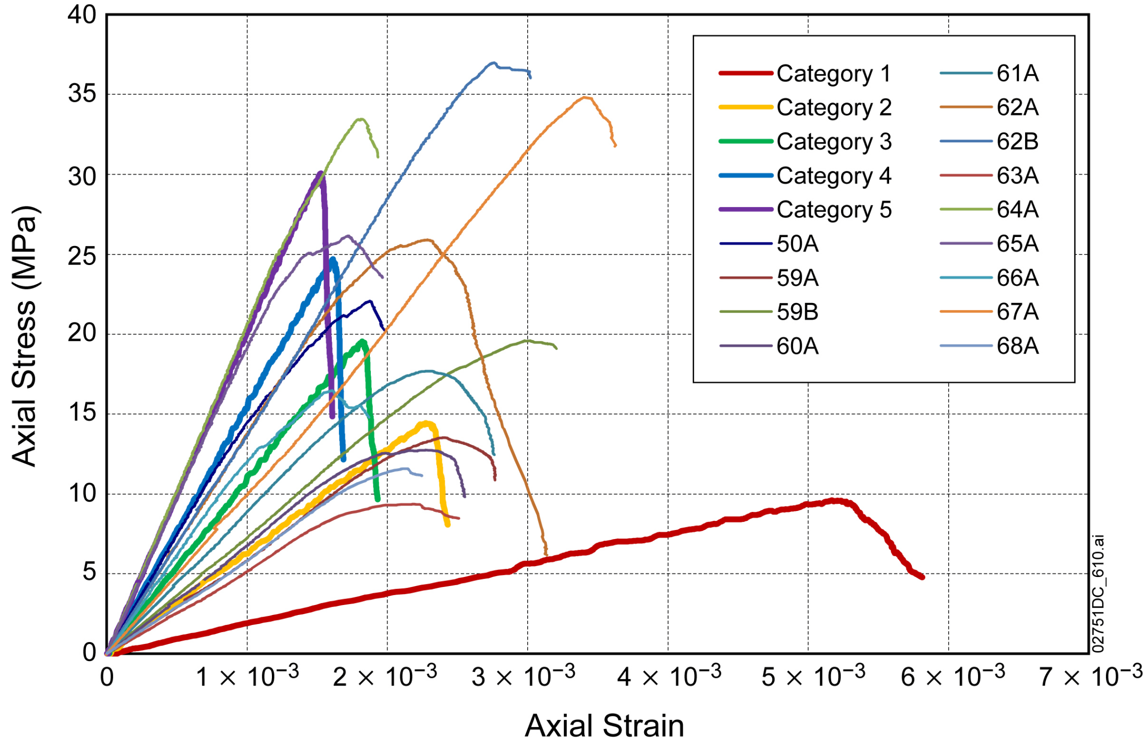

NOTE: Thick lines represent UDEC Voronoi block model data; thin lines represent the experimental data.

Figure 6. Comparison of Stress-Strain Curves Obtained from Tests on 11.4-Inch-Diameter Upper Lithophysal Samples with Responses of the Calibrated UDEC Voronoi Block Model (60A, 63A, 68A – 24°C saturated; 50A, 59A, 61A, 62A, 64A, 65A, 66A – 24°C room dry; 59B, 67A – 190°C dry; 62B – 200°C dry)

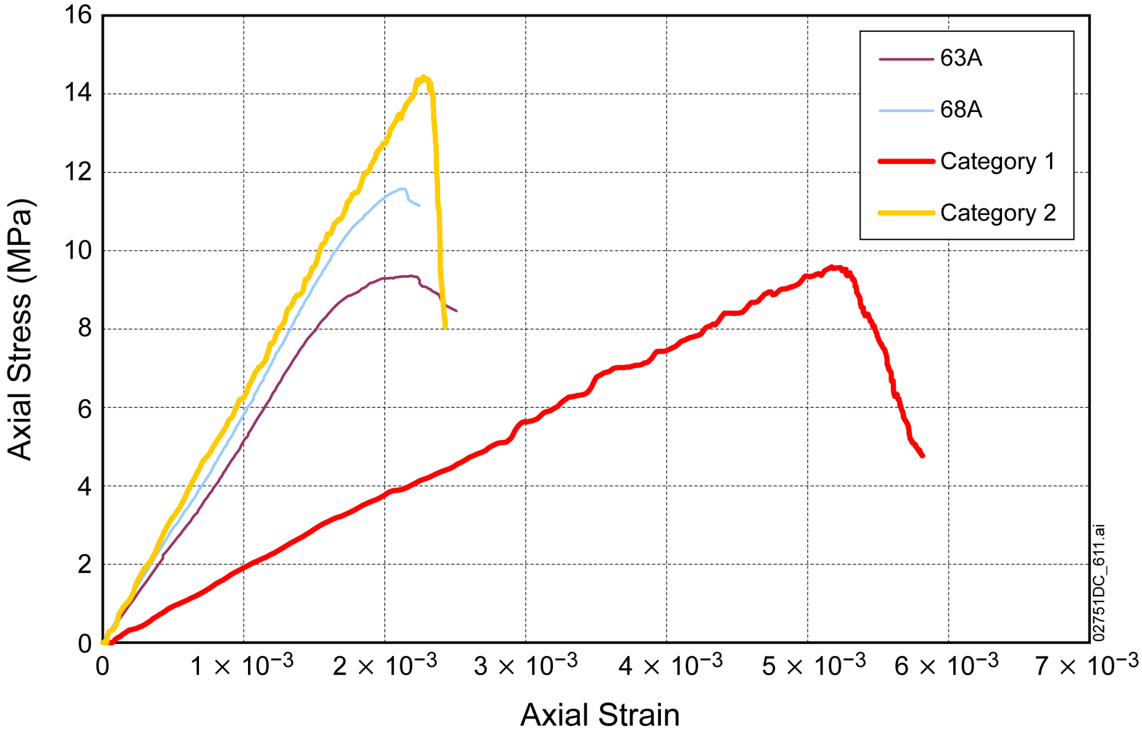

NOTE: Thick lines represent UDEC Voronoi block model data; thin lines represent the experimental data.

Figure 7. Comparison of Stress-Strain Curves Obtained from Tests on 11.4-Inch-Diameter Upper Lithophysal Samples with Responses of the Calibrated UDEC Voronoi Block Model for the Range of Rock Mass Qualities Corresponding to Categories 1 and 2 (63A, 68A – 24°C saturated)

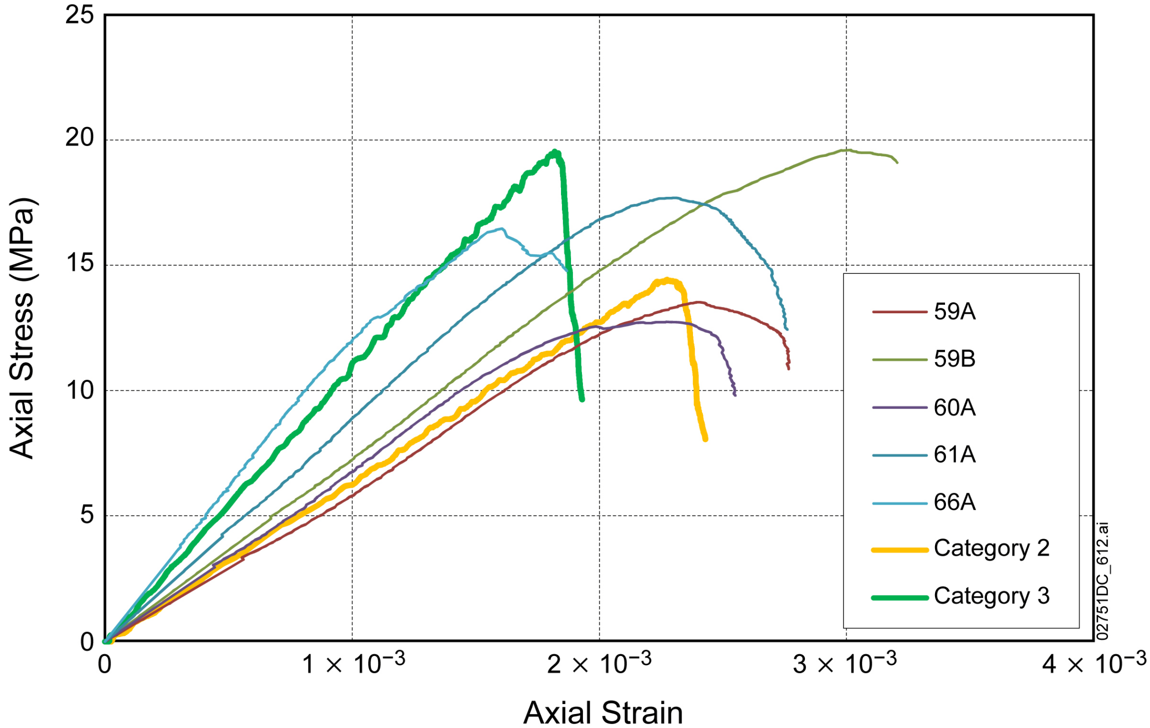

NOTE: Thick lines represent UDEC Voronoi block model data; thin lines represent the experimental data.

Figure 8. Comparison of Stress-Strain Curves Obtained from Tests on 11.4-Inch-Diameter Upper Lithophysal Samples with Responses of the Calibrated UDEC Voronoi Block Model for the Range of Rock Mass Qualities Corresponding to Categories 2 and 3 (60A – 24°C saturated; 59A, 61A, 66A – 24°C room dry; 59B – 190°C dry)

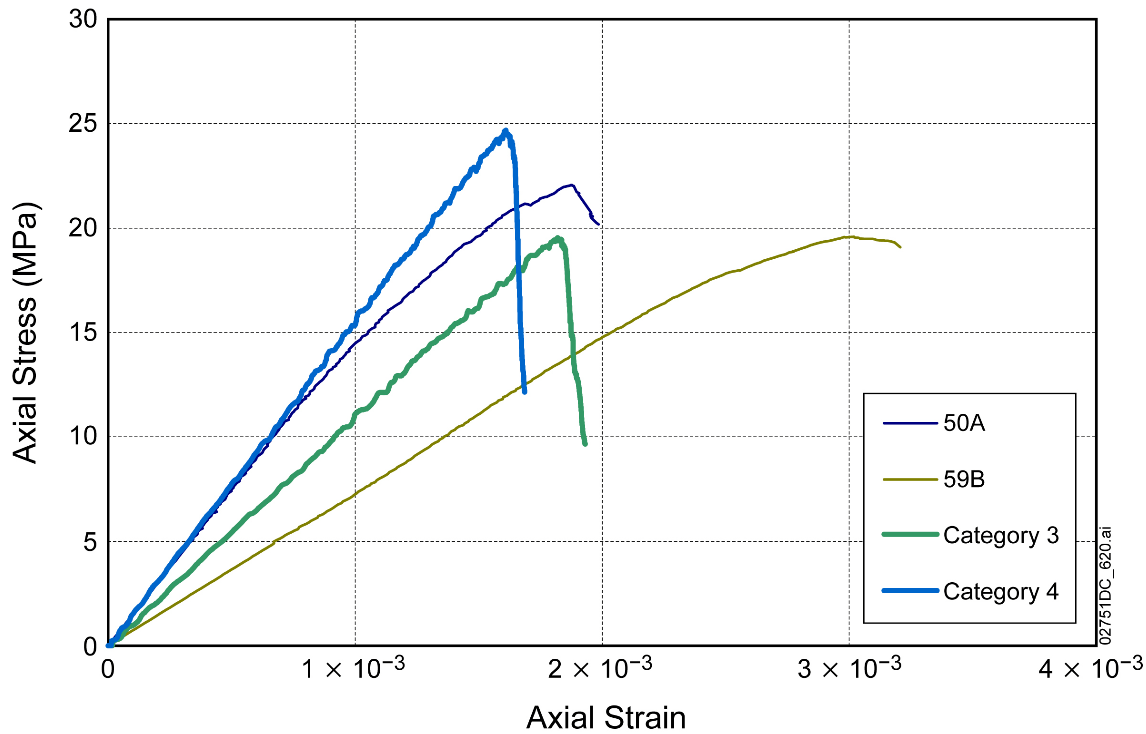

NOTE: Thick lines represent UDEC Voronoi block model data; thin lines represent the experimental data.

Figure 9. Comparison of Stress-Strain Curves Obtained from Tests on 11.4-Inch-diameter Upper Lithophysal Samples with Responses of the Calibrated UDEC Voronoi Block Model for the Range of Rock Mass Qualities Corresponding to Categories 3 and 4 (50A – 24°C room dry; 59B – 190°C dry)

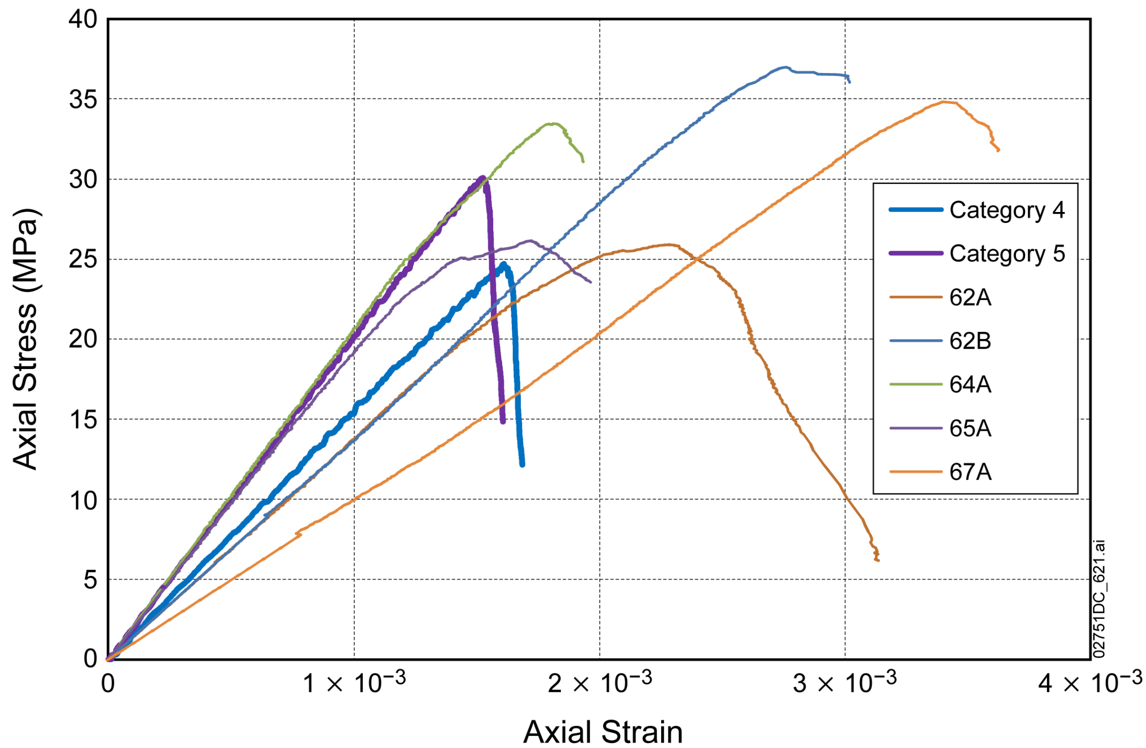

NOTE: Thick lines represent UDEC Voronoi block model data; thin lines represent the experimental data.

Figure 10. Comparison of Stress-Strain Curves Obtained from Tests on 11.4-Inch-Diameter Upper Lithophysal Samples with Responses of the Calibrated UDEC Voronoi Block Model for the Range of Rock Mass Qualities Corresponding to Categories 4 and 5 (62A, 64A, 65A – 24°C room dry; 67A – 190°C dry; 62B – 200°C dry)

1.4 CONCLUSIONS

The thorough and extensive sensitivity analysis of the effect of the variability and the uncertainty in the stiffness and strength of both upper and lower lithophysal on drift stability is carried out and documented in Section 6.4.2 of *Drift Degradation Analysis* (BSC 2004) and in the response to RAI 3.2.2.1.2.1-6-003. The five rock mass categories for the mean and the lower bound relations between stiffness and strength (BSC 2004, Figure E-13) cover and bound (providing expected and bounding responses) the loading responses (i.e., stiffness and strength) between the established limits. These limits were defined from the data collected in field and laboratory experiments on the lithophysal tuffs, as well as information gathered from detailed mapping of the lithophysal units within the Topopah Spring Member of the Paintbrush Tuff.

Another aspect of the modeling method was chosen to increase confidence in the bounding approach and to address the uncertainties in the post-peak part of the stress-strain curve. The stress-strain behavior of the lithophysal tuffs were modeled by a relatively abrupt loss of strength, immediately after the peak stress. However, the laboratory experiments on the lithophysal tuffs show that the post-peak strengths of the samples are characterized by a more gradual decrease in strength than in the models. The model approximation of the post-peak material response bounds observed responses from the test data resulting in overprediction of rockfall.

2. COMMITMENTS TO NRC

None.

3. DESCRIPTION OF PROPOSED LA CHANGE

None.

4. REFERENCES

BSC (Bechtel SAIC Company) 2004. *Drift Degradation Analysis*. ANL-EBS-MD-000027 REV 03. Las Vegas, Nevada: Bechtel SAIC Company. ACC: DOC.20040915.0010; DOC.20050419.0001.

Jaeger, J.C. and Cook, N.G.W. 1976. *Fundamentals of Rock Mechanics.* 2nd Edition. New York, New York: John Wiley & Sons.

Price, R.H. 1986. *Effects of Sample Size on the Mechanical Behavior of Topopah Spring Tuff.* SAND85-0709. Albuquerque, New Mexico: Sandia National Laboratories. ACC: NNA.19891106.0125.

Price, R.H. 1993. "Strength-Size-Porosity Empirical Model for Yucca Mountain Tuff." *EOS, Transactions (Supplement), 74,* (43), 571. Washington, D.C.: American Geophysical Union.

Price, R.H. and Bauer, S.J. 1985. "Analysis of the Elastic and Strength Properties of Yucca Mountain Tuff, Nevada." *Research & Engineering Applications in Rock Masses, Proceedings of the 26th U.S. Symposium on Rock Mechanics, Rapid City, South Dakota, June 26-28, 1985.* Ashworth, E., ed. Pages 89-96. Boston, Massachusetts: A.A. Balkema.

Price, R.H.; Martin, R.J., III; Boyd, P.J.; and Noel, J.S. 1994. "Mechanical and Bulk Properties in Support of ESF Design Issues." *High Level Radioactive Waste Management, Proceedings of the Fifth Annual International Conference, Las Vegas, Nevada, May 22-26, 1994. 4*, 1987-1992. La Grange Park, Illinois: American Nuclear Society.

Price, R. H.; Martin III, R.J.; Boyd, P.J.; and Boitnott, G.N. 1996. "Mechanical and Bulk Properties of the Intact Rock Collected in the Laboratory in Support of the Yucca Mountain Site Characterization Project." [*Proceedings of the] Workshop on Rock Mechanics Issues in Repository Design & Performance Assessment, Held at Holiday Inn Crowne Plaza Rockville, Maryland, September 19-20, 1994*. NUREG/CP-0150. Washington, D.C.: U.S. Nuclear Regulatory Commission.

Ross, C.S. and Smith, R.L. 1961. *Ash-Flow Tuffs: Their Origin, Geologic Relations, and Identification.* Professional Paper 366. Reston, Virginia: U.S. Geological Survey. ACC: NNA.19910405.0048.